Organic & Biomolecular Chemistry

RSC Publishing

PAPER

View Article Online
View Journal | View Issue

Cite this: *Org. Biomol. Chem.*, 2013, **11**, 8443

The self-assembly of cystine-bridged γ-peptide-based cyclic peptide–dendron hybrids†

Zhizhong Lin,[a,d] Liangchun Li,*[c] Yujin Yang,[a] Hongmei Zhan,[a] Yu Hu,[a] Zhiming Zhou,[c] Jin Zhu,[a] Qiwei Wang[a] and Jingen Deng*[b,e]

Received 16th March 2013,
Accepted 22nd October 2013

DOI: 10.1039/c3ob40532j

www.rsc.org/obc

Novel cystine-bridged γ-peptide-based cyclic peptide–dendron hybrids have been synthesized by oxidative coupling between two cysteine residues of the linear peptides *via* the formation of disulfide bonds in high yields. The self-assembly of the hybrids was studied by FT-IR, ^{1}H NMR, TEM, and AFM analyses which indicate that the nanotube was constructed through intermolecular hydrogen-bonding of the hydrophobic cyclic peptide moieties and possesses amphiphilic property by conjugating a hydrophilic dendron on the exterior of the cyclic peptide ring. The diameters of nanofibers that consisted of nanotubes depend on the employed solvent in the self-assembly process, and uniform filaments formed from double amphiphilic nanotubes *via* hydrophobic interactions between their hydrophobic faces have been observed in water as well as in aqueous solutions.

1 Introduction

Currently there is intense interest in the formation of nanostructures with technological or biomedical applications based on their self-assembly through the spontaneous interactions of their component molecules.[1,2] Cyclic peptides (CPs), due to their efficiency in limiting the conformational flexibility and ease in modulation of their three-dimensional (3D) structures, are one of the extensively studied self-assembly building blocks.[2–5] To date, cyclic D,L-α-peptides,[6,7] β-peptides,[8–10] δ-peptides,[11] and the hybrids including α- and γ- or ε-amino acids[12–16] have been applied to self-assemble into well-defined nanotubes. The majority of cyclic peptide nanotubes (CPNs) so far have hydrophilic inner surfaces and can only be permeated by polar molecules.[3,7,9,17] To further control the transport properties of a wide range of molecules through self-assembling peptide nanotubes (SPNs), artificial amino acids containing rigid cycloalkanes,[12–14] aromatic rings,[16,18] and unsaturated groups[11] have been used to modify the physical properties of the nanotube interior. Granja and co-workers[12–15] developed α,γ-cyclic peptide nanotubes consisting of alternating D-α-amino acids and (1*R*,3*S*)-3-aminocyclohexanecarboxylic acids (γ-Achs)[19] in which the C_2 methylene group of each cyclohexyl moiety is projected into the lumen of the cylinder, generating a partially hydrophobic cavity. The α,γ-CPNs favor the encapsulation of apolar solvents,[12,20,21] which shows potential applications in drug delivery.[17,22,23]

The main challenge in designing a self-assembling fibrous system is to control the assembly to form uniform reproducible structures. Recently, we reported that γ-CP composed of γ-Achs only self-assembled into γ-CPN, in which the projection of C_2 methylene of all γ-Achs into the lumen creates a more hydrophobic interior in the organic nanotubes.[24] Moreover, the dendritic side-chains can modulate the physical properties to improve the solubility of the γ-CP and control the aggregation of the CPNs in solvents, and also promote the stability of the CPN due to the aromatic π–π stacking interactions between adjacent dendrons upon association of the γ-CPs.[24,25] The side-chain functional groups of the cyclic peptide have an influence on the formation of either single-peptide nanotubes or higher-order 3D aggregates.[15,18,24,26] Peptide–dendron[27,28] and peptide–polymer[4,29–32] hybrids offer the potential to study how the conformational properties of two folded structural elements all allosterically communicate structural information. On the other hand, the self-assembly of amphiphilic components leading to microphase separation constitutes a powerful approach toward the fabrication of complex supramolecular architectures, especially tubular nanostructures due to both the hydrophobic and hydrophilic interactions.[27,28,33] Furthermore, for the applications in biomedicine and

[a]*Chengdu Institute of Organic Chemistry, Chinese Academy of Sciences, Chengdu 610041, China*
[b]*Key Laboratory of Drug-Targeting of Education Ministry, West China School of Pharmacy, Sichuan University, Chengdu 610041, China. E-mail: jgdeng@scu.edu.cn*
[c]*School of Life Science and Engineering, Southwest University of Science and Technology, Mianyang, 621010, China. E-mail: lilc76@gmail.com*
[d]*University of Chinese Academy of Sciences, Beijing, 100049, China*
[e]*Jiangxi Key Laboratory of Organic Chemistry, Jiangxi Science & Technology Normal University, Nanchang 330013, China*

†Electronic supplementary information (ESI) available: Scheme S1, Fig. S1–S22, complete experimental procedures, and characterization of cyclic peptide–dendron hybrids and spectral data. See DOI: 10.1039/c3ob40532j

biomaterials, it is desirable to be able to tailor pore sizes and pore surfaces of CPs. In our preliminary experiments, we were unsuccessful in synthesizing γ-CPs with larger pore diameter, such as cyclic γ-hexapeptides composed of homochiral or alternating chiral γ-Achs, although *N*-methylated cyclic γ-hexapeptides have been obtained.[34,35] It was reported that macropeptides have been conveniently prepared by the formation of a disulfide bond between two cysteine residues,[36,37] and the self-organization of cystine-based macrocycles facilitated the formation of the tubular nanostructures.[38–40] Herein, we would like to describe the synthesis and self-assembly behavior of novel disulfide-bond containing CP-dendron hybrids (Fig. 1, **1a** and **1b**) composed of a homochiral γ-tetrapeptide and one bridged cystine residue attached to hydrophilic dendritic side-chains on the exterior of the CP-ring.[24,34]

In our previous research, we found that a linear tetrapeptide consisting of only chiral γ-Achs has very poor solubility in common solvents. For increasing the solubility of the peptides, benzoates with branched Tg (triethylene glycol monomethyl ether) chains (Fig. 1) were chosen to modify the γ-CPs.[24] The synthesis of **1a** and **1b**, which are conjugated with the first- and second-generation hydrophilic dendrons respectively, will be performed by coupling two cysteine residues of the linear peptides on the basis of the formation of disulfide bonds.[36,37] Amphiphilic nanotubes can be formed from the self-assembly of **1a** and **1b** *via* β-sheet-like hydrogen-bond-mediated parallel stacking, respectively, on which a hydrophobic wall (both the inner and outer surfaces are hydrophobic) is constructed by the self-organization of γ-tetrapeptide moieties bearing hydrophobic cyclohexane backbones[12,21,24] (Fig. 2). Therefore, in an aqueous environment, the hydrophobic side of a single tube is completely buried against other hydrophobic tube faces to aggregate into bundles of CPNs due to the hydrophobic interactions, around which the hydrophilic dendritic side-chains like to project toward the aqueous media because of hydrate. We investigate the impact of different assembly methods and solvents on the overall nanoscale dimensions (*i.e.*, length and width), and we show that the diameters of nanofibers depend on the employed solvent in the self-assembly process. To the best of our knowledge, there has been no report that the aggregation of CPNs can be controlled using their amphiphilic characteristics.[1–4,41,42]

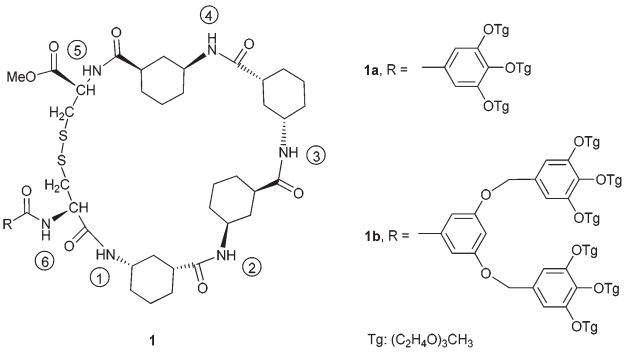

Fig. 1 The structures of **1a** and **1b**.

2 Results and discussion

The synthetic strategy is outlined in Scheme 1. Initially, for the synthesis of **1a** and **1b**,[43] the first- and second-generation dendritic benzoic acids were attached to the amino group of methyl L-cysteinate **2** respectively and subsequent deprotection was performed by hydrolysis of the methyl esters. (1*R*,3*S*)-Ach

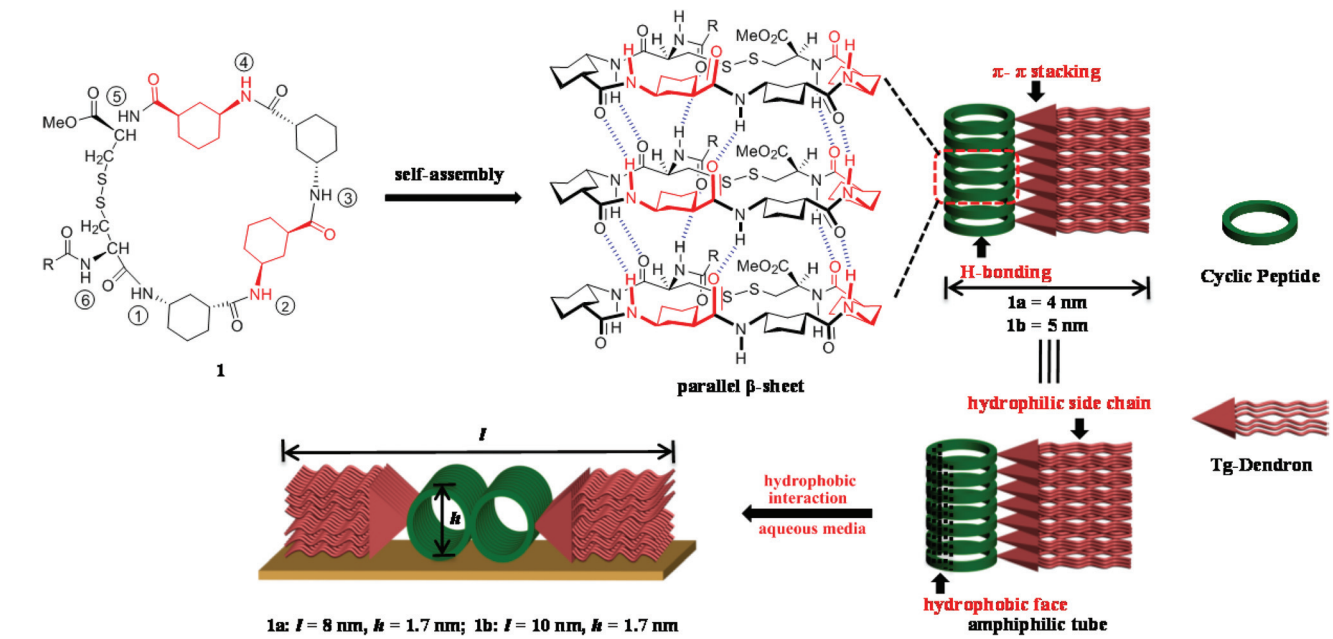

Fig. 2 Schematic representation of the hybrids **1** and their supramolecular stacking mediated by intermolecular hydrogen-bonding, shown by dotted lines. Cartoon representation showing the self-assembly of the hybrids **1** into amphiphilic nanotubes and then into nanofibers.

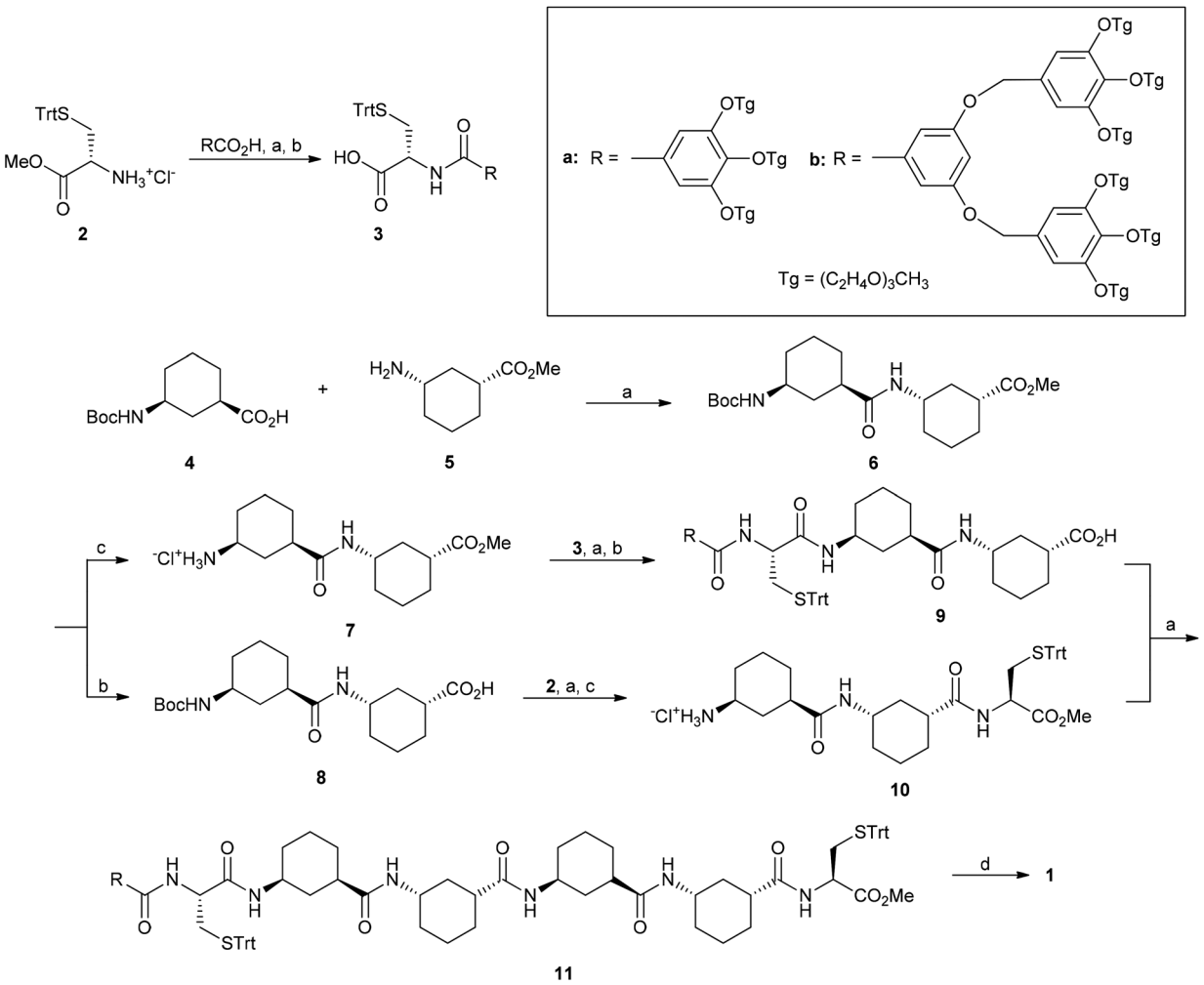

Scheme 1 Synthesis of **1**. (a) EDCI, HOBt, DIPEA, CH_2Cl_2; (b) LiOH, THF–H_2O–CH_3OH; (c) HCl (gas), CH_2Cl_2; (d) I_2, CH_3OH–CH_2Cl_2.

was prepared according to our method.[19] Boc-protected **4** and methyl protected **5** were prepared with the corresponding standard methods. Dipeptide **6** was obtained by coupling between acid **4** (Boc-γ-Ach-OH) and amine **5** (H-γ-Ach-OMe) with good yield. In the presence of EDCI, HOBt and DIPEA, the deprotected dipeptides **7** and **8** were coupled respectively with correspondingly modified cysteines **2** and **3**, giving the tripeptides **9** and **10**. The linear hexapeptides **11** that consisted of one cysteine residue grafted with the Tg-dendrons at the N-terminus, another cysteine residue at the C-terminus, and a γ-tetrapeptide constructed from four (1*R*,3*S*)-Ach residues in the middle were synthesized by coupling of **9** and **10** after respective deprotection. The cyclization of linear hexapeptides **11** proceeded by simple iodine oxidation between the cysteine residues, where side chains were protected with trityl groups, constructing desired disulfide bonds in one step, including both deprotection and oxidative coupling to lead to **1a** and **1b** in 73% and 49% yields, respectively.[36,37] The molecular structures of **1a** and **1b** were identified by NMR, IR, and HRMS analyses. Moreover, the formation of cyclic peptides was also confirmed by MALDI-TOF-MS analysis showing the corresponding mass signals for different ion adducts.[43] As expected, the second-generation dendron conjugated cyclic hexapeptide **1b** has better solubility than the first-generation one **1a** in common solvents such as $CHCl_3$ and CH_3CN, as well as aqueous solution.

The rod-like assemblies of **1a** were gained from ($CHCl_3$–CH_3OH) *via* vapor-phase diffusion (see ESI, Fig. S2†), but they are unsuitable for single-crystal X-ray diffraction. Fourier transform infrared (FT-IR) spectroscopy of **1a** in the solid state (Fig. S3†) shows a sharp peak at 1631.8 cm^{-1} in the amide I region, and 1535.8 cm^{-1} in the amide II region, which are characteristic of extensively hydrogen-bonding β-sheet-like networks.[44–46] Moreover, the N–H stretching frequency occurring at 3305.3 cm^{-1} also corresponds to tightly hydrogen bonded ring-stacked networks. These results suggest that the needle-shaped fibers are constructed from tightly packed nanotubes formed by self-assembly of **1a** on the basis of β-sheet-like hydrogen-bonding. These observations also prompted us to investigate the self-assembly behavior of **1a** and **1b** in the solutions.

A solution of **1a** in $CHCl_3$ (6 mg mL^{-1}) was equilibrated *via* vapor-phase diffusion against *n*-hexane, and colorless gels

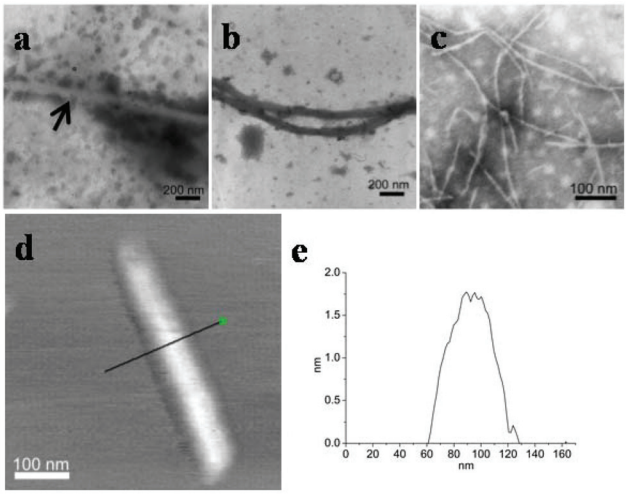

Fig. 3 (a–c) TEM images of the gels formed by **1a** and then dispersed in *n*-hexane, water and water–ethanol (1 : 1, v/v), respectively; (d) AFM images of the **1a** sample adsorbed on mica, showing nanofibers; (e) height profile measured along the line shown in (d).

were formed at room temperature for two days.[47] As the initial study, the organogels were dispersed in *n*-hexane by sonication. The resulting sample was dried on a carbon-coated copper TEM grid, which was then negatively stained with a phosphotungstic acid solution. Under these conditions, transmission electron microscopy (TEM) revealed the presence of long fibers with a width of about 100 nm (Fig. 3a). By dispersing the gels in pure water, a fibrous assembly of *ca.* 92 nm in diameter was obtained (Fig. 3b). When the gels of **1a** were dispersed in a mixture of water and ethanol (1 : 1, v/v), TEM studies revealed the presence of filaments with widths of about 8 nm (Fig. 3c). This dimension of the aggregate is approximately twice the extended molecular length (4 ± 0.5 nm in molecular length of **1a** by the Corey–Pauling–Koltun (CPK) molecular model).[33] The same sample was also determined by atomic force microscopy (AFM) and the AFM image showed the nanofiber with an average height of 1.75 nm that corresponds to the estimated width of a naked cyclic peptide of the hybrid **1** (1.7 ± 0.1 nm by the CPK model) (Fig. 3d–e and S4†). These results implied that the uniform filaments only consist of two nanotubes.

According to the same procedure, the gels of **1b** were prepared and dispersed in *n*-hexane;[47] TEM images showed long ribbon-like aggregates with diameters of 140–300 nm (Fig. 4a). When the gels were dispersed in pure water, in contrast to **1a** that formed fibers with a large diameter, **1b** showed cylindrical aggregates with diameters ranging from 8 nm to 10 nm (Fig. 4b). By considering the extended molecular lengths of **1b** (5 ± 0.5 nm by the CPK model), the images indicate that the diameter of cylindrical aggregates corresponds to double the molecular length. By dispersing the gels of **1b** in water–ethanol (1 : 1, v/v), TEM images displayed discrete filaments of about 6 nm and 10 nm in diameter, respectively (Fig. 4c respectively shows black and white arrows). Furthermore, the

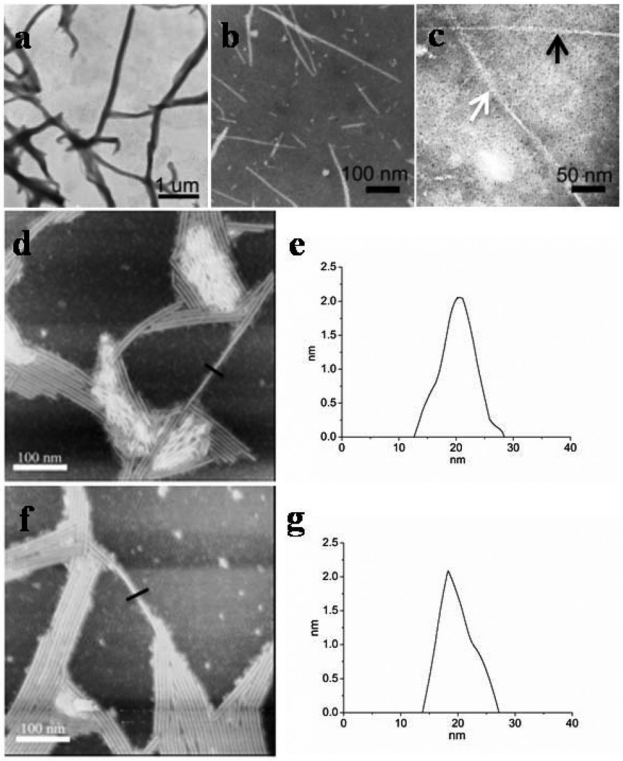

Fig. 4 (a–c) TEM images of the gels formed by **1b** and then dispersed in *n*-hexane, water and water–ethanol (1 : 1, v/v), respectively. (d, f) AFM images of the gels of **1b** dispersed in water and water–ethanol (1 : 1, v/v), showing nanofibers; (e, g) height profile measured along the line shown in (d, f).

samples were investigated by AFM and the AFM images indicated the formation of filaments with a uniform diameter and an average height of 2.06 nm (Fig. 4d–e and S5†) and 2.04 nm (Fig. 4f–g and S6†) for the gels of **1b** dispersed in water and water–ethanol (1 : 1, v/v) respectively, suggesting that the second-generation benzyl ether-dendron bearing hydrophilic Tg-chains could impact the height of the filaments by comparing with the result of **1a** (Fig. 2). Thus the TEM and AFM images revealed that nanostructures of **1b** dispersed in water–ethanol (1 : 1, v/v) exist in both individual nanotubes and bundles of only two nanotubes, but in water only fibrous bundles consisting of two nanotubes exist.

Self-assembling in aqueous media is of particular interest for applications in biomedicine.[1,41,48–51] Amphiphilic components, especially those bearing EG (ethylene glycol) chains, have shown an interesting property of enhanced self-assembly into a variety of nanostructures in aqueous media.[1,41] In this work, for improving the solubility of CPs, the hybrid **1b** conjugated with the second-generation dendritic Tg-chains was synthesized and shows good solubility in aqueous solution.[24] Thus, **1b** was dissolved in acetonitrile, water, and their mixture (water–CH_3CN, 5 : 95; v/v) respectively by heating and the resulting transparent solution was cooled to room temperature overnight. TEM studies were carried out on a copper grid. When the self-assembly of **1b** was performed in pure acetonitrile, visual formation of the hybrid assemblies occurred

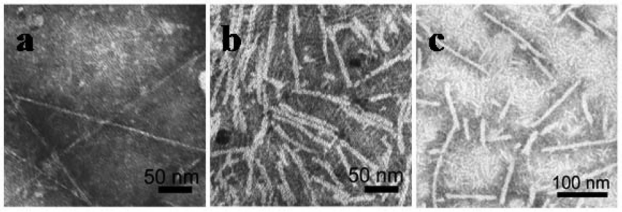

Fig. 5 TEM images of the tubular nanostructures formed by the self-assembly of **1b** in CH_3CN (a), 5% H_2O in CH_3CN (b), and H_2O (c).

under these conditions. TEM images showed uniform fibrils with a diameter of about 5 nm and more than 430 nm in length (Fig. 5a), which corresponded to an individual columnar structure of the nanotube organized from **1b** on the basis of β-sheet-like hydrogen-bonding (Fig. 2). In a mixture of 5% water in CH_3CN, fibrous assemblies of about 10 nm in diameter were observed and a maximum length could be roughly estimated with more than 110 nm (Fig. 5b). Notably, in pure water, highly uniform filaments of 10 nm in diameter with a shorter length (size ranging from 45 to 180 nm) were also found by TEM analysis (Fig. 5c), which is in good agreement with double size of the molecular length of **1b**, suggesting that the filaments consisted of only two nanotubes.

These results indicate that the hybrid **1** composed of a CP-ring bearing a hydrophobic γ-tetrapeptide moiety and a hydrophilic dendritic pendant may self-assemble into well-ordered and amphiphilic tubular nanostructures on the basis of intermolecular hydrogen-bonding of the CP-rings. Further aggregation of the amphiphilic nanotubes depends on the employed solvent system. In the nonpolar $CHCl_3$–*n*-hexane system, both hybrids **1a** and **1b** formed a bundle of nanofibers, which can be dispersed in a mixture of water and ethanol (1 : 1, v/v) as uniform filaments consisting of two or single amphiphilic nanotubes because of solvation of Tg-side chains to suppress lateral aggregation.[24] It is interesting that only **1b** can be dispersed in water to form uniform filaments of double amphiphilic nanotubes. In the polar CH_3CN, only a single nanotube self-assembled from the hybrid **1b** was observed. In pure water or even mixing a small amount of water (5%) into the CH_3CN phase, double tubular nanostructures were only formed from **1b**. However, the nanofibers became shorter with the addition of water probably because of the competition by water for CP–CP intermolecular hydrogen-bonding sites hindering further organization of nanotubes.[21,52] In aqueous solution, amphiphilic nanotubes especially self-assembled from **1b** *via* β-sheet-like hydrogen-bonding were further organized from individual nanotubes into double tubular nanostructures in order to decrease the exposure of the hydrophobic faces of the amphiphilic nanotubes to aqueous media. Two amphiphilic nanotubes possess an inherent tendency to hold together by strong hydrophobic interactions between the hydrophobic faces of neighboring tubes in aqueous solution, and the sufficient hydration of the dendritic Tg-chains attached to other faces of the tubes suppresses the lateral aggregation (Fig. 2).

^1H NMR spectroscopy was then used to probe the aggregation tendency of the hybrids **1** in solution. The spectrum of **1a** even in the polar solvent DMSO-d_6 displays poor-resolved signals (Fig. S13†), showing the strong intermolecular aggregation. Notably, in DMSO-d_6, ^1H NMR spectrum of **1b** is sharp with well-resolved signals (Fig. 6a)[43] and 2D NOESY analysis (Fig. S14 and S15†) shows that the N–H and C_α–H bonds of adjacent cyclohexane rings as well as cysteine residue are in a *cis* relationship, as shown in Fig. 2 and Fig. S1.† Fortunately, in $CDCl_3$, the spectrum of **1b** shows peaks that broaden obviously but also well-defined and significant concentration-dependent chemical shifts, suggesting that the N–H groups participate in hydrogen-bonding interaction for the

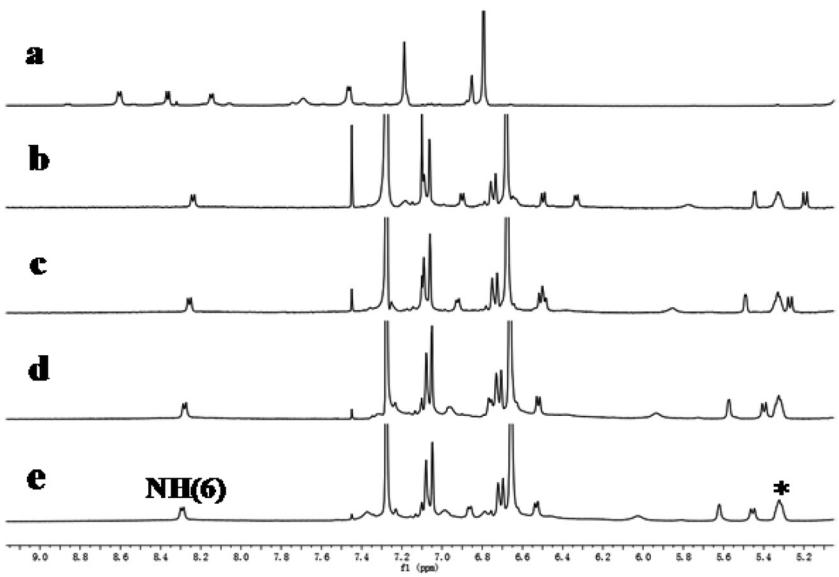

Fig. 6 Selected region of ^1H NMR spectra of **1b** (a) in DMSO-d_6, (b) 2 mM, (c) 10 mM, (d) 20 mM, and (e) 40 mM in $CDCl_3$, showing the downfield shifts of N–H signals. The "*" sign denotes the C_α–H signal in cysteine residues (5.32 ppm).

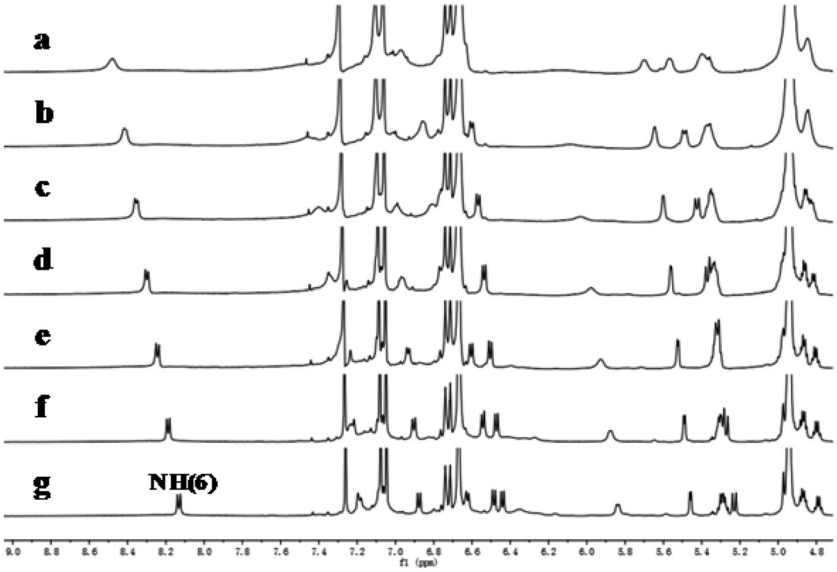

Fig. 7 Temperature dependence of the ^{1}H NMR spectrum of 10 mM of **1b** in $CDCl_3$ (a, −10 °C; b, 0 °C; c, 10 °C; d, 20 °C; e, 30 °C; f, 40 °C; g, 50 °C), showing the upfield shifts of N–H signals.

intermolecular organization, although the presence of slowly interconverting conformers on the NMR time scale indicates that there are more than six peaks for the N–H groups (Fig. 6b–e). Moreover, the N–H signal assigned as the exocyclic amide proton (NH(6), also see: Fig. 2) in the downfield (8.24 ppm, in 2 mM solution in $CDCl_3$) only displays 0.05 ppm downfield shift on increasing the concentration to 40 mM, which implies that the exocyclic amide formed a stable intermolecular hydrogen-bonding.[13] ^{1}H NMR spectra of the hybrid **1b** in $CDCl_3$ at lower temperature show broad signals in the amide proton region indicating that the hybrid **1b** formed intermolecular hydrogen-bonding (Fig. 7a and 7b). With the elevation of temperature, these chemical shift values move to upfield from 8.48 to 8.13 ppm and the signals become more and more well-resolved, suggesting weakening of the hydrogen-bonding (Fig. 7).

Solution FT-IR investigations furnished additional evidence of self-assembled β-sheet structures in the nanotubes (Fig. 8, Table 1; also see: Fig. S7–12†).[24,46,48,49,53] The observed N–H stretching frequencies (amide A bands) of 3302 and 3301 cm^{-1} for **1a** in $CHCl_3$ and **1b** in CH_3CN respectively indicate tightly intermolecular hydrogen-bonding. The FT-IR measurement also shows amide I bands at 1636–1638 cm^{-1} and amide II bands at 1537–1539 cm^{-1} for **1a** in $CHCl_3$, **1b** in CH_3CN and D_2O that are characteristic of nanotubes formed from β-sheet-like networks. In contrast to the result of FT-IR analysis for **1a** in $CHCl_3$, the FT-IR spectrum of **1b** in $CHCl_3$ displays the amide I band at 1649 cm^{-1} and amide II band at 1508 cm^{-1} (Fig. 8c, also see Table 1) that are not consistent with a typical β-sheet structure, in which the band at 1649 cm^{-1} is fairly similar to the random coil peak[54,55] (around 1654 cm^{-1}) and the peak at 1508 cm^{-1} is located in the regions of nonbonding amide II bands (1503–1516 cm^{-1}) observed in the $CHCl_3$ solutions.[53] The FT-IR analysis for **1a** shows that there is a strong tendency

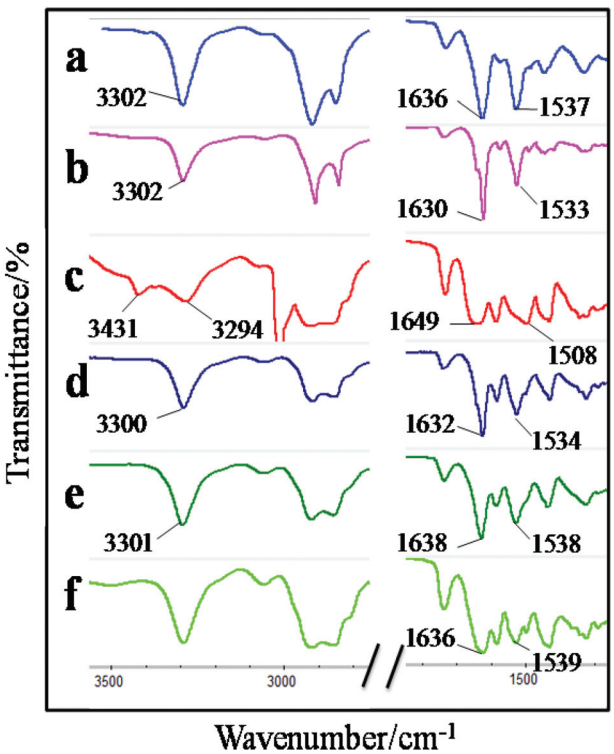

Fig. 8 Selected region of FT-IR spectra of **1a** (a) in $CHCl_3$ and (b) in the gel state and FT-IR spectra of **1b** (c–f) in $CHCl_3$, gel state, CH_3CN and D_2O, respectively.

to aggregate in $CHCl_3$, probably as a result of aromatic π–π stacking interactions between the adjacent first-generation dendrons on the exterior of CP[24] as well as from the intermolecular hydrogen-bonding between the exocyclic amides of **1a** (Fig. 2 and S1a†). However, the steric hindrance between the

Table 1 Absorption frequencies of hybrids in different media

Compounds	Solvents[a]	Frequencies [cm^{-1}]		
		Amide A[b]	Amide I	Amide II
1a	$CHCl_3$	3302	1636	1537
	Gels	3302	1630	1533
1b	$CHCl_3$	3294 (3431)	1649	1508
	Gels	3300	1632	1534
	CH_3CN	3301	1638	1538
	D_2O	[c]	1636	1539

[a] The concentrations of the samples in solutions were 10 mM for both **1a** in $CHCl_3$ and **1b** in D_2O. The concentrations of **1b** in both $CHCl_3$ and CH_3CN were 20 mM. [b] Values in parentheses are for putative amide bands arising from non-hydrogen-bonding NH. [c] It is impossible to subtract the solvent absorption in this region because of the strong ν (O–D) band of water.

second-generation dendritic Tg-chains conjugated on the exterior of CP of **1b**, especially after the solvation of Tg-chains in $CHCl_3$, may inhibit the association of **1b** to form intermolecular hydrogen-bonds and thereby the β-sheet structures.[30,32] The addition of *n*-hexane resulted in the decrease of the solvation of the dendritic Tg-chains and hence triggers the aggregation process to form organogels. Really, in contrast to the $CHCl_3$ solution, the FT-IR spectrum of **1b** for the gels formed in a mixture of $CHCl_3$ and *n*-hexane exhibits the characteristic amide I and II bands at 1632 and 1534 cm^{-1} respectively for β-sheet hydrogen-bonding (Fig. 8d and Table 1). The CP-rings of **1** can self-assemble by stacking on top of one another through contiguous parallel or antiparallel β-sheet-like hydrogen-bonding on either side. As shown in Fig. 2 and Fig. S1,† five inter-ring hydrogen-bonds might form between the cyclic hexapeptides of **1** with an exocyclic hydrogen-bond between the dendritic amides in the parallel model (Fig. 2 and S1a†), while only four intermolecular hydrogen-bonds exist in the antiparallel models (Fig. S1b–c†). Moreover, in the antiparallel models, the exocyclic hydrogen-bonding cannot proceed due to the γ-Ach residue shift of one unit toward the right or left. These suggest that the parallel stacking of hybrids **1** is energetically much more favorable than the antiparallel ones. In particular, this is supported by the fact that the exocyclic amide proton (NH(6)) signal gradually upfield shifts on increasing the temperature from −10 to 50 °C (Fig. 7), and the amide IA absorptions at 1636–1638 cm^{-1}, in the absence of the characteristic amide IB bands at 1680–1695 cm^{-1}, imply the formation of a parallel β-sheet conformation in the nanotubes.[24,46,53]

3 Conclusions

In summary, we have studied the self-assembly of cystine-bridged γ-peptide-based cyclic peptide–dendron hybrids **1a** and **1b**, which were conveniently synthesized by oxidative coupling between two cysteine residues of the linear peptides on the basis of the formation of disulfide bonds in high yields. ^{1}H NMR and FT-IR analyses show that **1a** and **1b** can self-assemble by β-sheet-like hydrogen-bond-mediated parallel stacking between cyclic hexapeptides of the hybrids. TEM as well as AFM measurements reveal that width-controllable nanofibers consisting of a single or two nanotubes have been obtained by self-assembling, and the diameter of nanofibers depends on the employed solvent in the self-assembly process. Especially, the hybrid **1b** conjugated with the second-generation benzyl ether-dendron bearing hydrophilic Tg-chains possesses good solubility in common solvents and has self-assembled into highly uniform nanofibers in polar solvents. Shorter nanofibers were formed in water or aqueous acetonitrile. These results indicate that the integration of dendritic EG chains and hydrophobic cyclic peptides in the amphiphilic nanotubes may allow the control of the width as well as length of the nanofibers aggregated by β-sheet-like hydrogen-bonding between the cyclic hexapeptides of the hybrids. Moreover, the design of introducing disulfide-bonds into the cyclic γ-peptides might permit control over the pore diameter simply by adjusting the number of γ-Achs subunits.[38] We believe that uniform nanofibers have potential applications in nanotechnological fields such as drug delivery and catalysis. Further investigation on this issue is currently being carried out to better understand the conformation of analogous γ-peptides and potential transport/carrier applications.

4 Experimental

General

(1*R*,3*S*)-3-Aminocyclohexanecarboxylic acid (γ-Ach) was prepared according to our method.[19] *O*-(7-Azabenzotriazol-1-yl)-1,1,3,3-tetramethyluronium hexafluorophosphate (HATU), 1-hydroxy-7-azabenzotriazole (HOAT), 1-hydroxybenzotriazole (HOBt) and *N*-(3-dimethylaminopropyl)-*N*-ethylcarbodiimide hydrochloride (EDCI) were all used as obtained from GL Biochem (Shanghai) Ltd. All other reagents obtained from commercial suppliers were used without further purification unless otherwise noted. Dichloromethane (DCM) was dried and distilled over calcium hydride. Analytical thin-layer chromatography was performed on silica gel GF254 plates from Qingdao Haiyang Chemical Co. Ltd. Silica gel flash chromatography was performed using silica gel (200–300 mesh) from Qingdao Haiyang Chemical Co. Ltd. Melting points were recorded on a BÜCHI Melting Point B-545 apparatus and are uncorrected. Optical rotations were measured with an automatic Perkin-Elmer 341 digital polarimeter; concentrations are given in g per 100 mL. Proton nuclear magnetic resonance (^{1}H NMR) spectra were recorded on Bruker WM-300 MHz or 600 MHz spectrometers. Chemical shifts are reported in parts per million (ppm, δ) from TMS or solvent resonance as the internal standard. ^{1}H NMR splitting patterns are designated as singlet (s), doublet (d), triplet (t), and quartet (q). All first-order splitting patterns were assigned on the basis of the appearance of the multiplet. Splitting patterns that could not be easily interpreted are designated as multiplet (m) or broad (br). Carbon nuclear magnetic resonance (^{13}C NMR) spectra were recorded on Bruker WM-300 MHz or 600 MHz

spectrometers. Electrospray (ESI) mass spectra were recorded on a Bruker BioTOF Q mass spectrum.

Synthesis of cyclic peptide–dendron hybrids.[43] *Synthesis of* **1a**: To a solution of I_2 (101 mg, 0.4 mmol) in CH_3OH–CH_2Cl_2 (10 : 90, 120 mL), **11a** (30 mg, 0.017 mmol) in CH_3OH–CH_2Cl_2 (10 : 90, 30 mL) was added dropwise at −10 °C, and the resulting mixture was stirred at −10 °C for 20 minutes. After 2 M $Na_2S_2O_3$ (100 mL) was added, the reaction mixture was concentrated. The solution was extracted with $CHCl_3$ (3 × 30 mL). The combined organic layers were dried over $MgSO_4$ and concentrated *in vacuo*. The residue was purified by column chromatography on silica gel ($CHCl_3$–CH_3OH = 30 : 1, v/v) to give **1a** (16 mg, 73%) as a white solid. Mp: decomposed at 278 °C; $[\alpha]_D^{20}$ = −12 (*c* = 0.2, $CHCl_3$–MeOH = 3 : 1, v/v); FT-IR (ν/cm^{-1}): 3443, 3296, 2932, 2859, 1747, 1634, 1582, 1546, 1496, 1452, 1397, 1334, 1218, 1112; ESI-HRMS, calculated for $C_{63}H_{102}N_6Na_2O_{20}S_2$ $[M + 2Na]^{2+}$: 686.3913; found 686.3187; MS (MALDI-TOF), calculated for $C_{63}H_{102}N_6NaO_{20}S_2$ $[M + Na]^+$: 1349.6; found 1349.8.

Synthesis of **1b**: To a solution of I_2 (594 mg, 2.34 mmol) in CH_3OH–CH_2Cl_2 (10 : 90, 400 mL), **11b** (251.3 mg, 0.1 mmol) in CH_3OH–CH_2Cl_2 (10 : 90, 100 mL) was added dropwise at −10 °C, and the resulting mixture was stirred at −10 °C for 4 hours. After 2 M $Na_2S_2O_3$ (100 mL) was added, the reaction mixture was concentrated to remove organic solvents. Then, the solution was extracted with $CHCl_3$ (3 × 50 mL). The combined organic layers were dried over anhydrous Na_2SO_4 and concentrated *in vacuo*. The residue was purified by column chromatography on silica gel ($CHCl_3$–CH_3OH = 40 : 1, v/v) to give **1b** (99 mg, 49%) as a white solid. Mp: decomposed at 271 °C; $[\alpha]_D^{20}$ = −16 (*c* = 0.2, CH_2Cl_2); ^{1}H NMR (DMSO-d_6, 600 MHz, ppm), δ 1.23–1.35 (m, 16H), 1.64–1.91 (m, 16H), 2.07–2.37 (m, 4H), 2.99–3.16 (m, 4H), 3.20, 3.22 (2 × s, 18H), 3.38–3.42 (m, 12H), 3.48–3.58 (m, 27H), 3.65–3.72 (m, 15H), 4.00 (brs, 4H), 4.09 (brs, 8H), 4.56–4.66 (m, 2H), 5.00 (s, 4H), 6.77 (s, 4H), 6.83 (s, 1H), 7.16 (s, 2H), 7.42–7.43 (m, 2H, NH), 7.65 (br s, 1H, NH), 8.10 (d, 1H, NH, *J* = 6.5 Hz), 8.32 (d, 1H, NH, *J* = 7.7 Hz), 8.56 (d, 1H, NH, *J* = 8.0 Hz); ^{13}C NMR (DMSO-d_6, 150 MHz, ppm), δ 23.26, 24.08, 24.41, 28.16, 28.29, 30.88, 31.39, 31.74, 32.05, 35.59, 35.72, 36.13, 43.15, 44.23, 44.80, 47.47, 47.72, 48.34, 51.50, 52.53, 53.05, 58.49, 68.91, 69.49, 70.09, 70.21, 70.32, 70.45, 71.75, 72.28, 105.40, 107.06, 107.54, 132.47, 136.33, 137.76, 152.65, 159.83, 166.00, 168.96, 171.33, 173.76, 173.94, 174.37, 174.98; FT-IR (ν/cm^{-1}): 3436, 3307, 3056, 2931, 2863, 1746, 1635, 1593, 1535, 1505, 1439, 1347, 1332, 1296, 1249, 1112, 941, 846; ESI-HRMS, calculated for $C_{98}H_{156}KN_6O_{34}S_2$ $[M + K]^+$: 2064.0; found 2063.9; MS (MALDI-TOF), calculated for $C_{98}H_{156}NaN_6O_{34}S_2$ $[M + Na]^+$: 2048.0; found 2048.5.

Preparation of cyclic peptide nanotubes and nanofibers for transmission electron microscopy (TEM) analysis:

Method A: 3 mg of **1a** or **1b** was dissolved in $CHCl_3$ (0.5 mL) and equilibrated *via* vapor-phase diffusion against 5 mL of *n*-hexane, resulting in a gel phase after 2–4 days. The gels were dispersed in *n*-hexane, water and water–ethanol (1 : 1, v/v), respectively, by sonication.

Method B: **1b** was dissolved in acetonitrile or water or their mixture (0.1 mg mL^{-1}), and then heated in an oil bath at 100 °C to yield a transparent solution. The water content in acetonitrile was 5% (v/v). The resulting solution of **1b** was cooled to room temperature overnight.

Transmission electron microscopy (TEM). After the sample for TEM was prepared, droplets of 10 μL of the solution were placed on the specimen holder, a 200 mesh copper grid. After 2 min, the grid was stained with 1% (w/v) phosphotungstic acid for 1 min and the excess fluid was removed. Samples were viewed using a HITACHI H-600 electron microscope for TEM at an accelerating voltage of 75 kV.

Atom force microscopy (AFM) measurements. After the gels were dispersed in water or a water–ethanol (1 : 1, v/v) mixture, 10 μL of the suspension was deposited on a freshly cleaved piece of mica and left to adhere overnight. AFM imaging was performed at room temperature using the tapping mode on a Seiko SPI3800N. According to the manufacturer, the probes used were etched silicon probes with a typical tip radius of <10 nm; the normal spring constant was 3 N m^{-1}. The drive frequency was around 75 kHz.

Solution FT-IR measurements. FT-IR measurements were performed with the $CHCl_3$ and CH_3CN solution placed in a 0.1 mm KBr solution IR cell, and the D_2O solution was measured in a CaF_2 cell. All samples were recorded on a NICOLET 6700 FT-IR Spectrometer.

Acknowledgements

We thank the National Natural Science Foundation of China (grant no. 91027022, 21002099 and 20428202), the National Basic Research Program of China (973 Program, no. 2010CB833300), and Sichuan University for financial support of the research. The Chengdu Institute of Organic Chemistry, Chinese Academy of Sciences, and West China School of Pharmacy, Sichuan University, contributed equally to this work.

Notes and references

1 H.-J. Kim, T. Kim and M. Lee, *Acc. Chem. Res.*, 2011, **44**, 72–82.
2 D. T. Bong, T. D. Clark, J. R. Granja and M. R. Ghadiri, *Angew. Chem., Int. Ed.*, 2001, **40**, 988–1011.
3 R. J. Brea, C. Reiriz and J. R. Granja, *Chem. Soc. Rev.*, 2010, **39**, 1448–1456.
4 R. Chapman, M. Danial, M. L. Koh, K. A. Jolliffe and S. Perrier, *Chem. Soc. Rev.*, 2012, **41**, 6023–6041.
5 D. Seebach and J. Gardiner, *Acc. Chem. Res.*, 2008, **41**, 1366–1375.
6 M. R. Ghadiri, J. R. Granja, R. A. Milligan, D. E. McRee and N. Khazanovich, *Nature*, 1993, **366**, 324–327.
7 M. R. Ghadiri, J. R. Granja and L. K. Buehler, *Nature*, 1994, **369**, 301–304.

8 D. Seebach, J. Matthews, A. Meden, T. Wessels, C. Baerlocher and L. McCusker, *Helv. Chim. Acta*, 1997, **80**, 173–182.
9 T. D. Clark, L. K. Buehler and M. R. Ghadiri, *J. Am. Chem. Soc.*, 1998, **120**, 651–656.
10 F. Fujimura, M. Fukuda, J. Sugiyama, T. Morita and S. Kimura, *Org. Biomol. Chem.*, 2006, **4**, 1896–1901.
11 D. Gauthier, P. Baillargeon, M. Drouin and Y. L. Dory, *Angew. Chem., Int. Ed.*, 2001, **40**, 4635–4638.
12 M. Amorin, L. Castedo and J. R. Granja, *J. Am. Chem. Soc.*, 2003, **125**, 2844–2845.
13 R. Brea, L. Castedo and J. R. Granja, *Chem. Commun.*, 2007, 3267–3269.
14 C. Reiriz, M. Amorin, R. Garcia-Fandino, L. Castedo and J. R. Granja, *Org. Biomol. Chem.*, 2009, **7**, 4358–4361.
15 C. Reiriz, R. J. Brea, R. Arranz, J. L. Carrascosa, A. Garibotti, B. Manning, J. M. Valpuesta, R. Eritja, L. Castedo and J. R. Granja, *J. Am. Chem. Soc.*, 2009, **131**, 11335–11337.
16 W. S. Horne, C. D. Stout and M. R. Ghadiri, *J. Am. Chem. Soc.*, 2003, **125**, 9372–9376.
17 J. R. Granja and M. R. Ghadiri, *J. Am. Chem. Soc.*, 1994, **116**, 10785–10786.
18 R. Hourani, C. Zhang, R. van der Weegen, L. Ruiz, C. Li, S. Keten, B. A. Helms and T. Xu, *J. Am. Chem. Soc.*, 2011, **133**, 15296–15299.
19 Y. Hu, S. L. Yu, Y. J. Yang, J. Zhu and J. G. Deng, *Chin. J. Chem.*, 2006, **24**, 795–799.
20 M. Amorin, L. Castedo and J. R. Granja, *Chem.–Eur. J.*, 2005, **11**, 6543–6551.
21 R. García-Fandiño, J. R. Granja, M. D'Abramo and M. Orozco, *J. Am. Chem. Soc.*, 2009, **131**, 15678–15686.
22 Y.-b. Lim, E. Lee and M. Lee, *Angew. Chem., Int. Ed.*, 2007, **46**, 3475–3478.
23 H. Liu, J. Chen, Q. Shen, W. Fu and W. Wu, *Mol. Pharm.*, 2010, **7**, 1985–1994.
24 L. Li, H. Zhan, P. Duan, J. Liao, J. Quan, Y. Hu, Z. Chen, J. Zhu, M. Liu, Y.-D. Wu and J. Deng, *Adv. Funct. Mater.*, 2012, **22**, 3051–3056.
25 E. R. Zubarev, E. D. Sone and S. I. Stupp, *Chem.–Eur. J.*, 2006, **12**, 7313–7327.
26 T. Nakanishi, H. Okamoto, Y. Nagai, K. Takeda, I. Obataya, H. Mihara, H. Azehara, Y. Suzuki, W. Mizutani, K. Furukawa and K. Torimitsu, *Phys. Rev. B: Condens. Matter*, 2002, **66**, 165417.
27 V. Percec, A. Dulcey, V. Balagurusamy, Y. Miura, J. Smidrkal, M. Peterca, S. Nummelin, U. Edlund, S. Hudson, P. Heiney, H. Duan, S. Magonov and S. Vinogradov, *Nature*, 2004, **430**, 764–768.
28 H. Shao and J. R. Parquette, *Angew. Chem., Int. Ed.*, 2009, **48**, 2525–2528.
29 J. Couet, J. D. J. S. Samuel, A. Kopyshev, S. Santer and M. Biesalski, *Angew. Chem., Int. Ed.*, 2005, **44**, 3297–3301.
30 M. Ten Cate, N. Severin and H. Börner, *Macromolecules*, 2006, **39**, 7831–7838.
31 T. Xu, N. Zhao, F. Ren, R. Hourani, M. T. Lee, J. Y. Shu, S. Mao and B. A. Helms, *ACS Nano*, 2011, **5**, 1376–1384.
32 R. Chapman, M. L. Koh, G. G. Warr, K. A. Jolliffe and S. Perrier, *Chem. Sci.*, 2013, **4**, 2581–2589.
33 J. H. Ryu, N. K. Oh and M. Lee, *Chem. Commun.*, 2005, 1770–1772.
34 Z. Chen, L. Li, M. Lv, J. Zhu and J. Deng, in *Peptides: Chemistry, Biology and Pharmaceutical Sciences*, ed. R. Wang and K.-R. Wang, Chemical Industry Press, 2011, pp. 54–57.
35 A. Guerra, R. J. Brea, M. Amorin, L. Castedo and J. R. Granja, *Org. Biomol. Chem.*, 2012, **10**, 8762–8766.
36 A. Cuthbertson and B. Indrevoll, *Org. Lett.*, 2003, **5**, 2955–2957.
37 S. Kitada, S. Fujita, Y. Okada, S. Kim and K. Chiba, *Bioorg. Med. Chem. Lett.*, 2011, **21**, 4476–4479.
38 D. Ranganathan, V. Haridas, C. S. Sundari, D. Balasubramanian, K. P. Madhusudanan, R. Roy and I. L. Karle, *J. Org. Chem.*, 1999, **64**, 9230–9240.
39 D. Ranganathan, M. P. Samant and I. L. Karle, *J. Am. Chem. Soc.*, 2001, **123**, 5619–5624.
40 V. Haridas, S. Sahu and A. R. Sapala, *Chem. Commun.*, 2012, **48**, 3821–3823.
41 J. H. Ryu, D. J. Hong and M. Lee, *Chem. Commun.*, 2008, 1043–1054.
42 Y. Ishihara and S. Kimura, *J. Pept. Sci.*, 2010, **16**, 110–114.
43 For further details, see ESI.†
44 J. D. Hartgerink, J. R. Granja, R. A. Milligan and M. R. Ghadiri, *J. Am. Chem. Soc.*, 1996, **118**, 43–50.
45 C. Toniolo and M. Palumbo, *Biopolymers*, 1977, **16**, 219–224.
46 B. Jagannadh, M. S. Reddy, C. L. Rao, A. Prabhakar, B. Jagadeesh and S. Chandrasekhar, *Chem. Commun.*, 2006, 4847–4849.
47 The S–S bond-linked hybrids **1a** and **1b** are stable under the self-assembly conditions, which has been conformed by HPLC and MALDI-TOF-MS analyses, see ESI (Fig. S19–22†).
48 S. Matsumura, S. Uemura and H. Mihara, *Mol. BioSyst.*, 2005, **1**, 146–148.
49 S. Guha, M. G. B. Drew and A. Banerjee, *Chem. Mater.*, 2008, **20**, 2282–2290.
50 Y.-b. Lim, K.-S. Moon and M. Lee, *Chem. Soc. Rev.*, 2009, **38**, 925–934.
51 X. Zhao and S. Zhang, *Macromol. Biosci.*, 2007, **7**, 13–22.
52 T. D. Clark, J. M. Buriak, K. Kobayashi, M. P. Isler, D. E. McRee and M. R. Ghadiri, *J. Am. Chem. Soc.*, 1998, **120**, 8949–8962.
53 N. Yamada, K. Ariga, M. Naito, K. Matsubara and E. Koyama, *J. Am. Chem. Soc.*, 1998, **120**, 12192–12199.
54 M. Reches and E. Gazit, *Science*, 2003, **300**, 625–627.
55 P. I. Haris and D. Chapman, *Biopolymers*, 1995, **37**, 251–263.